

The Higgs-Amplitude mode in the optical conductivity in the presence of a supercurrent: Gauge invariant formulation

Ke Wang,^{1,2} Rufus Boyack,³ and K. Levin¹

¹*Department of Physics and James Franck Institute, University of Chicago, Chicago, Illinois 60637, USA*

²*Kadanoff Center for Theoretical Physics, University of Chicago, Chicago, Illinois 60637, USA*

³*Department of Physics and Astronomy, Dartmouth College, Hanover, New Hampshire 03755, USA*

Observing the amplitude-Higgs mode in superconductors has been a central challenge in condensed matter physics. Unlike the phase mode in the electromagnetic (EM) response, the amplitude mode is not needed to satisfy gauge invariance. Indeed, it couples to linear EM response properties only in special superconductors that are associated with a pairing vector $\mathbf{Q} \neq 0$. In this paper we characterize the amplitude-mode contribution within a gauge-invariant treatment of the linear optical conductivity for these non-uniform superconductors, noting that they are by their very nature particularly vulnerable to pair-breaking from non-magnetic impurities. This leads to inevitable damping of the Higgs mode. Our gauge-invariant formulation provides an in-depth understanding of two sets of f -sum rules which must be obeyed. We illustrate how difficult it is to disentangle the neutral amplitude mode contributions from those of the charged quasi-particles. These observations are presented in the context of an applied supercurrent, where we observe a new low-frequency feature that reflects the superfluid density and appears consistent with recent experiments.

Introduction. Superconductivity and gauge invariance are inextricably connected, not just in condensed matter physics but also in high-energy physics. This observation dates back to Nambu¹, who introduced the concept of Nambu-Goldstone bosons² and pointed out that the electromagnetic (EM) response in a superconductor^{3,4} must reflect phase-mode excitations of the order parameter. This saga continued through the work of Anderson⁵, who noted that, in general, superconductors would also have amplitude-mode excitations, (now called the ‘‘Higgs’’ mode to adopt the particle-physics nomenclature^{6–9}) which at the time were not thought to be readily visible⁴.

More recently^{10,11}, we have come to understand that there is a way to observe the amplitude mode in condensed matter experiments, beginning with the work of Littlewood and Varma¹² and our own group¹³ (Levin and Browne) who considered special kinds of superconductors with a co-existent charge-density wave. But more common than that are superconductors which carry a supercurrent. A calculation of the EM response for such a system must respect gauge invariance and charge conservation. But it is easy to miss^{14–16} the amplitude mode if one is not careful. It cannot be ignored, however, and will generally enter into the response of a non-uniform superconductor. This occurs generically through the characteristic wave vector \mathbf{Q} , which enables a linear coupling to the EM field through terms involving the vector potential \mathbf{A} , of the form $\mathbf{A} \cdot \mathbf{Q}$ ¹⁷.

This paper addresses how the amplitude mode shows up in the AC conductivity when a supercurrent associated with a characteristic wave vector \mathbf{Q} is present and what are the implications for experiment. We emphasize at the outset that it is essential to have a gauge invariant formulation of the conductivity. Without gauge invariance, the calculated optical conductivity violates charge conservation. We note that there are earlier schemes^{18,19} which utilize the Eilenberger-Usadel approach, and although these are thought to be quite important, they may suffer from inconsistencies with gauge invariance^{20–22}.

In a gauge invariant formalism one has to incorporate all

possible couplings of the current to the vector potential at a linear response level. The approach we use here was developed by Kulik *et al.*²³. By contrast with a uniform superconductor, where the Higgs mode is undamped at zero wave vector and independent of impurity effects, in a non-uniformly paired superconductor or in the presence of a supercurrent where there is broken time-reversal symmetry, the Higgs mode is sensitive to inevitable non-magnetic impurities^{24,25}. While this greatly increases the complexity, this problem is of sufficient importance with implications for experimental devices as well¹⁹, that it merits close examination.

We emphasize that the figures in this paper underline an essential difficulty in disentangling the Higgs contribution from other terms that appear in the conductivity. There are two distinct components of the current: (i) that due to the quasi-particles, and (ii) that from the Higgs modes. These two contributions are surprisingly similar as we demonstrate. This suggests that it is generally hard to isolate the Higgs contribution in experiments. Nevertheless, here we are able to do so theoretically, which it is hoped will inform future experiments.

Gauge-invariant linear response. We now provide the theoretical details of the linear-response formalism²³, that includes the phase and amplitude fluctuations of the order parameter. Fundamental to linear response theory is the EM kernel $K^{\mu\nu}$, which describes how the four-vector current $J^\mu = (\rho, \mathbf{J})$ responds to a weakly applied external EM field $A^\mu = (\phi, \mathbf{A})$:

$$J^\mu(q) = K^{\mu\nu}(q)A_\nu(q). \quad (1)$$

Here $q = (q_0, \mathbf{q})$ is a four-vector momentum. The invariance of the current under the gauge transformation $A_\mu \rightarrow A_\mu + \partial_\mu \lambda$ necessitates that $q_\mu K^{\mu\nu} = 0$, which is a crucial condition for a consistent linear response theory.

One can further decompose the kernel into

$$K^{\mu\nu}(q) = K_0^{\mu\nu}(q) + K_1^{\mu\nu}(q). \quad (2)$$

Here, K_1 accounts for the collective amplitude and phase motion of the condensate of Cooper pairs. K_0 reflects the

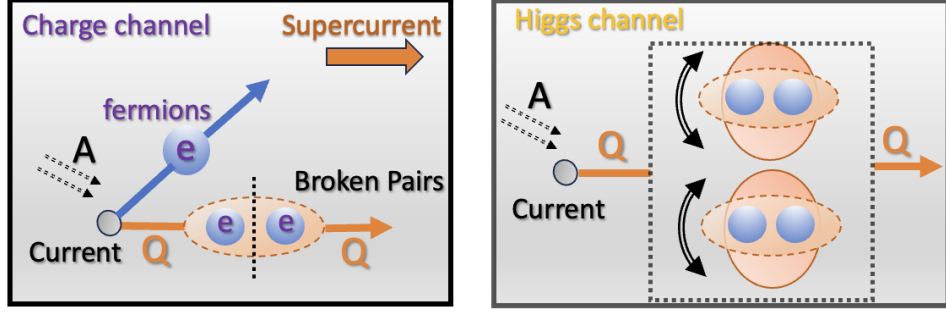


FIG. 1. Two contributions to the conductivity when a supercurrent is present. Charge channel on the left: The dashed arrows represent the incident electromagnetic (EM) field. The current has two contributions: one component (blue line) originates from fermions, as described in the Mattis-Bardeen conductivity, while the other component (orange line) arises from pair-breaking processes induced by the supercurrent and disorder. Right (see Eq(6)): \mathbf{Q} enables a coupling between the neutral Higgs mode and the current. Black solid arrows depict the collective motion of the order parameter (Higgs mode). Consequently, the charge channel contribution incorporates the effects of broken pairs, leading to behavior that closely resembles contributions from the Higgs channel, as illustrated in subsequent figures.

fermionic channel, where

$$K_0^{\mu\nu}(q) = P^{\mu\nu}(q) + \frac{ne^2}{m} G^{\mu\nu}. \quad (3)$$

The retarded current-current correlation function is defined in real space as $P^{\mu\nu}(t, \mathbf{x}) \equiv -i\theta(t)\langle [\hat{j}^\mu(t, \mathbf{x}), \hat{j}^\nu(0, 0)] \rangle$ where \hat{j} is the current operator. Here $G^{\mu,\nu}$ is a 4×4 diagonal tensor whose diagonal elements are $(0, 1, 1, 1)$, representing a diamagnetic contribution.

To derive the K_1 response, we implement a matrix linear-response approach²³ in which the perturbation of the condensate $\Delta_1 + i\Delta_2$ is included as additional contributions to the perturbing external field. These external fields $(A_\mu, \Delta_1, \Delta_2)$ cause a non-zero current $\langle j_\mu \rangle$ and order parameters $-g\langle \hat{\eta}_{1/2} \rangle/2$. Here $\hat{\eta}_i$ is the superconductor pairing field defined by $\Psi^\dagger(t, \mathbf{x})\tau_i\Psi(t, \mathbf{x})$, where $\Psi \equiv (\psi_\uparrow, \psi_\downarrow)^T$, $\psi_{\uparrow/\downarrow}$ is the spin-up/down fermionic operator, τ_i is the i -th Pauli matrix and g is the attractive s-wave interaction strength. For convenience, we let $\mu = 0, \dots, 3$, and $i = 1, 2$. Eliminating $\Delta_{1,2}$ leads to^{26,27}

$$K_1^{\mu\nu}(q) = - \sum_{i,j=1}^2 R^{\mu i}(q) \left(S + \frac{2}{g} \right)_{ij}^{-1} R_t^{j\nu}(q). \quad (4)$$

Here R and R_t are the cross correlation function between the current operator and the superconductor pairing field, $2/g$ relates to the interaction strength, and S is a correlation function involving the two superconductor pairing fields. The real-space definitions are given by $R^{\mu i}(t, \mathbf{x}) = -i\theta(t)\langle [j^\mu(t, \mathbf{x}), \hat{\eta}_i(0, 0)] \rangle$, $R_t^{i\mu}(t, \mathbf{x}) = R^{\mu i}(-t, -\mathbf{x})$, and $S_{ij}(t, \mathbf{x}) = -i\theta(t)\langle [\hat{\eta}_i(t, \mathbf{x}), \hat{\eta}_j(0, 0)] \rangle$, with $i, j = 1, 2$.²⁸

For all but strongly interacting superconductors, we can presume particle-hole symmetry around the Fermi surface so that the mixing term between phase and amplitude vanishes (i.e., $S_{12} = 0$). In this scenario, contributions from phase and amplitude fluctuations of order parameters can be separately

written as

$$K_{\text{phase}}^{\mu\nu} = - \frac{R^{\mu 2} R_t^{2\nu}}{S_{22} + 2/g}, \quad (5)$$

$$K_{\text{Higgs}}^{\mu\nu} = - \frac{R^{\mu 1} R_t^{1\nu}}{S_{11} + 2/g}. \quad (6)$$

It follows that one can construct two separate gauge-invariant components for the response tensor: $K_{\text{charge}} \equiv K_0 + K_{\text{phase}}$ and K_{Higgs} , where K_{charge} includes fermion dynamics and phase fluctuations.

We now prove gauge invariance of the two response tensors in a clean system, and then later we will address the more complicated proof for the dirty case. We start from the Ward-Takahashi identity (WTI) representing $U(1)$ symmetry in Nambu space^{29,30}:

$$\tau_3 G_0^{-1}(p_+) - G_0^{-1}(p_-)\tau_3 = q_\mu \gamma^\mu + 2i\Delta\tau_2. \quad (7)$$

Here G_0 is the fermionic propagator, $p_\pm = p \pm q/2$, $\gamma^\mu = (\tau_z, \mathbf{p}\tau_0)$ and Δ is the order parameter. One can use the WTI to prove the following identities:

$$q_\mu K_0^{\mu\nu}(q) = -2i\Delta R^{2\nu}, \quad (8)$$

$$q_\mu R^{\mu i}(q) = -2i\Delta \left(S_{2i} + \frac{2}{g}\delta_{2i} \right). \quad (9)$$

With these equations, it follows that

$$q_\mu K_{\text{charge}}^{\mu\nu} = 0, \quad q_\mu K_{\text{Higgs}}^{\mu\nu} = 0. \quad (10)$$

The fact that there are two separately gauge-invariant response tensors reflects the statement that there are two separately conserved charges. Since the Higgs modes are neutral excitations, the charge involved in K_{charge} is the total charge of the system while the charge in the Higgs channel is zero.

Turning to a more physical understanding, in Fig. 1, we illustrate the way these two terms K_{charge} and K_{Higgs} contribute to the conductivity and how they appear to have similar frequency structure. This observation depends on pronounced

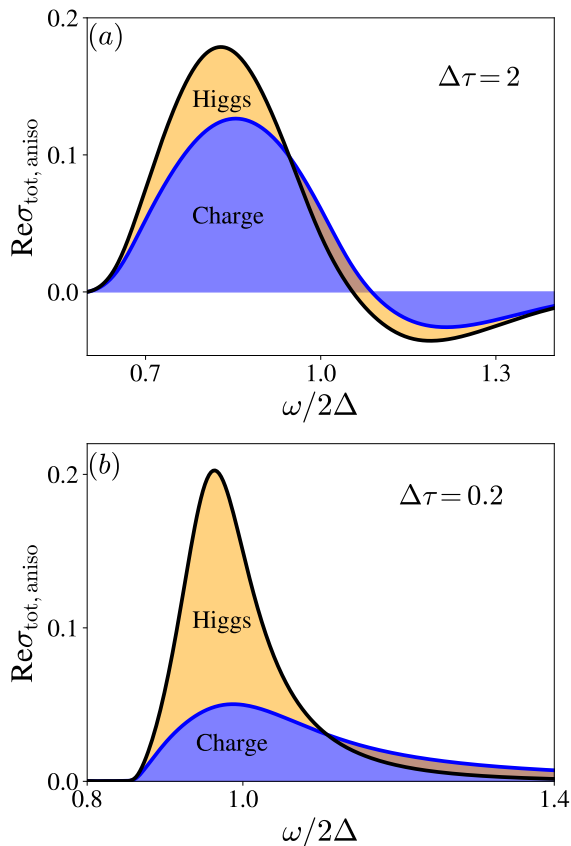


FIG. 2. Plot of the decomposition of the *total anisotropic* component of the conductivity given by $\sigma_{\text{tot,aniso}} = \hat{Q}_i \sigma_{\text{tot}}^{ij} \hat{Q}_j - \hat{Q}_i^\perp \sigma_{\text{tot}}^{ij} \hat{Q}_j^\perp$ in units of $\sigma_0 = e^2 m k_F / (2\pi^2 \hbar)$, where \hat{Q}^\perp is an arbitrary unit vector perpendicular to \hat{Q} . The supercurrent momentum is chosen as $k_F Q / m = \Delta/2$. (a) Contrary to the claim in Ref. 18 that only the Higgs component is anisotropic, we find that the charge component (which includes quasi-particle currents and phase fluctuations) also exhibits anisotropy and can even dominate over the Higgs component in cleaner samples ($\Delta\tau > 1$). In this regime, both the anisotropic charge and Higgs components display a negative tail at $\omega > 2\Delta$. (b) At the boundary separating clean and dirty samples ($\Delta\tau = 1$), the contributions from the Higgs and charge components become comparable. (c) As the system becomes dirtier ($\Delta\tau < 1$), the Higgs component dominates the peak of the anisotropic conductivity near 2Δ . For $\omega > 2\Delta$ there is a tail in the anisotropic conductivity which primarily originates from the charge component.

disorder effects as will be addressed in more detail later. As shown in the figure on the left, the charge channel in the presence of the supercurrent and disorder, contains a new term which depends on the superconducting amplitude. This is nevertheless distinct from the Higgs mode, as it is associated with charge effects and more particularly with the contribution to the current from impurity-derived broken Cooper pairs. By contrast, the figure on the right characterizes the way in which the neutral Higgs mode enters into the electromagnetic response, via coupling of the form $\mathbf{A} \cdot \mathbf{Q}$, as is seen in Eq(6).

Summary of central results. It is useful at this point to summarize some of the central results of this paper which are

related to the mechanisms in Fig. 1, before presenting all theoretical details. In Fig. 2, we show the anisotropic contribution to conductivity, decomposed into charge and Higgs sectors. We plot the difference between the parallel and perpendicular components of the total conductivity, represented by $\hat{Q}_i \sigma_{\text{tot}}^{ij} \hat{Q}_j - \hat{Q}_i^\perp \sigma_{\text{tot}}^{ij} \hat{Q}_j^\perp$, with \hat{Q}^\perp as a unit vector perpendicular to \hat{Q} . We argue that plotting this difference better highlights the Higgs contribution than comparing the total conductivity with and without a supercurrent¹¹. The latter case involves a conventional Mattis-Bardeen³¹ contribution, but we emphasize that this does not accurately represent the isotropic component σ_{iso} , as this too depends on the supercurrent.

This intimate connection between the charge and Higgs contributions should be evident in these figures as they can be seen to have most of their structure in a similar frequency range. This makes it extremely difficult to disentangle the Higgs from the background charge contribution. We also see that the Higgs contribution can be larger or smaller than this anisotropic charge component, depending on the degree of disorder. The relative size of the two contributions reflects their distinct dependence on disorder (see Ref. 32). One should note as well that the Higgs peak does not precisely align with 2Δ . It is affected as well by the excitation gap Δ_{ex} which is distinct from the order parameter. Finally, we note that the anisotropic charge component is assumed to be zero in earlier literature¹⁸, while we find here that it plays a major role in the electrodynamics. With extreme disorder it will, however, become progressively smaller than the Higgs contribution to the real part of the anisotropic conductivity. Importantly, however, this charge component can be quite significant when it comes to the imaginary part of the anisotropic conductivity, as we will see below.

Two *f-sum* rules. We now turn to calculations of the conductivity tensor which lead to these results and depend on the response tensor:

$$\sigma^{ij}(\omega) = \frac{ie^2}{\omega} K^{ij}(\omega, \mathbf{q} = 0). \quad (11)$$

Here $1 \leq i, j \leq 3$ denote three Cartesian directions. One can construct two gauge-invariant contributions to the conductivity σ_{charge} and σ_{Higgs} corresponding to K_{charge} and K_{Higgs} . As a consequence of gauge invariance, these are importantly associated with separate sum rules. In the presence of a supercurrent, we write the conductivity as a sum of two terms involving the “charge” contribution which involves the currents and the phase degrees of freedom and the Higgs which involves the amplitude fluctuation:

$$\sigma_{\text{tot}}(\omega) = \sigma_{\text{charge}}(\omega) + \sigma_{\text{Higgs}}(\omega) \quad (12)$$

We further decompose this “charge” contribution into isotropic (iso) and anisotropic (aniso) components and make the same decomposition for the superfluid densities associated with the charge component, which are of the form n_{iso} and n_{aniso} . Below, we adopt the units $\hbar = k_B = m = e = 1$.

Thus, we can write the conductivity associated with the

charge sector as :

$$\begin{aligned} \text{Re}\sigma_{\text{charge}}^{ij}(\omega) &= \pi\delta(\omega) \left(\delta_{ij}n_{\text{iso}} - \hat{Q}_i|n_{\text{aniso}}|\hat{Q}_j \right) \\ &+ \left(\delta_{ij}\sigma_{\text{iso}} + \hat{Q}_i\sigma_{\text{aniso}}\hat{Q}_j \right). \end{aligned} \quad (13)$$

Here, $\hat{Q} = \mathbf{Q}/|\mathbf{Q}|$ is a unit vector. The first term, $\propto \delta(\omega)$, represents the contribution from the condensate electrons, while the second term describes the conductivity at finite frequencies, as measured in experiments. The f -sum rule for the charge component leads to:

$$\int \frac{d\omega}{\pi} \text{Re}\sigma_{\text{iso}} = n - n_{\text{iso}}; \quad \int \frac{d\omega}{\pi} \text{Re}\sigma_{\text{aniso}} = +|n_{\text{aniso}}|. \quad (14)$$

Note that the anisotropic superfluid density n_{aniso} enters as a negative weight³³.

For the Higgs mode, which has only anisotropic contributions, we have

$$\text{Re}\sigma_{\text{Higgs}}^{ij}(\omega) = -\pi\delta(\omega)\hat{Q}_i|n_{\text{Higgs}}|\hat{Q}_j + \hat{Q}_i\sigma_{\text{Higgs}}\hat{Q}_j. \quad (15)$$

The f -sum rule associated with the Higgs contribution is given by $\int d\omega \text{Re}\sigma_{\text{Higgs}}/\pi = |n_{\text{Higgs}}|$. As with the anisotropic contribution to the charge contribution, the presence of the Higgs depresses the superfluid density and enters as a negative superfluid weight.

Effects of non-magnetic disorder. In the presence of a supercurrent which breaks time-reversal symmetry, all disorder leads to pairbreaking^{24,25}. This will affect the self consistent conditions for the central parameters in the theory (the current and the gap) as well as the electrodynamics.

The mean-field Hamiltonian in the presence of a supercurrent can be written in terms of Pauli matrices as

$$H(\mathbf{p}) = \mathbf{p} \cdot \mathbf{Q} + \xi(\mathbf{p})\tau_z + \Delta\tau_x. \quad (16)$$

Here, ξ represents the fermionic dispersion. We consider non-magnetic impurities which enter through the term $V(\mathbf{r})\tau_z$ and presume a contact interaction for this disorder. The self energy, evaluated in the Born approximation, is given by $\Sigma(p) = (2\pi)^{-3} \int d^3\mathbf{k} V(\mathbf{k})G(p-k)V(-\mathbf{k})$. The (inverse) fermion Green's function is then given by $G^{-1}(p) = G_0^{-1}(p) - \Sigma(p)$ with $G_0(i\omega_0, \mathbf{p}) = [i\omega_0 - H(\mathbf{p})]^{-1}$. Once the Greens function is known, one can determine derived quantities such as the order parameter Δ , the current J , and the single particle excitation gap Δ_{ex} which is distinct from the order parameter.

Disorder has a profound effect on the electrodynamic response which enters through a Bethe-Salpeter equation:

$$\begin{aligned} \Gamma(p_+, p_-) &= \gamma(p_+, p_-) + \int \frac{d^3k}{(2\pi)^3} V(k)\tau_z G(p'_+) \\ &\times \Gamma(p'_+, p'_-) G(p'_-) \tau_z V(-k), \quad p'_\pm = p_\pm + k. \end{aligned} \quad (17)$$

Here, $\gamma(p_+, p_-)$ represents a bare (vertex) operator while $\Gamma(p_+, p_-)$ is its renormalized version.

As an example, we consider the impurity vertex function for the current operator and denote its renormalized version by $\Gamma_{J,i}$, with $i = 1, 2, 3$. For details see Ref.32. Then, with all

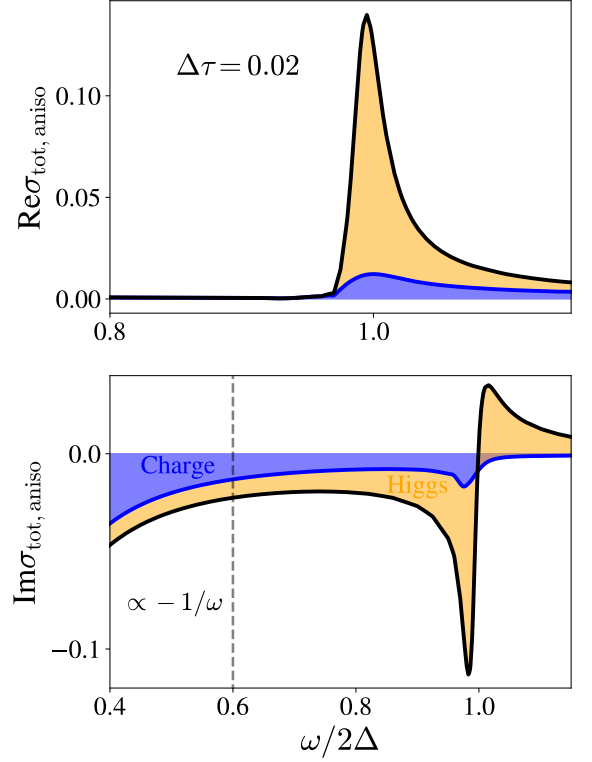


FIG. 3. (Color online). The effects of increasing disorder. Plots of the real and imaginary components of $\sigma_{\text{tot,aniso}}$ in units of σ_0 . In the imaginary contribution, an asymmetric feature appears around $\omega = 2\Delta$ and at even lower $\omega < \Delta$, a negative asymptote proportional to $-1/\omega$ emerges, reflecting a negative superfluid weight.

the impurity-renormalized vertices known, one can derive the full set of correlation functions Q , R , R_t , and S . For example, the current-current correlation function is

$$Q_0^{\mu\nu}(k) = T \sum_{i p_0} \int \frac{d^3p}{(2\pi)^3} j_\mu G(p) \Gamma_{J,\nu} G(p-k). \quad (18)$$

The evaluation of R , R_t , and S proceeds in a similar way, where either one of two vertex operators is replaced by its renormalized version.

Finally, we are able to prove the Ward-Takahashi identity in the presence of disorder. It can be shown that Eq. 7 generalizes to :

$$\tau_3 G^{-1}(p_+) - G^{-1}(p_-) \tau_3 = q^\mu \Gamma_{J,\mu} - 2i\Gamma_2 \Delta. \quad (19)$$

Using this identity, one can verify that Eqs. 8 and 9 remain valid, and consequently, so does Eq. 10. Thus, we have derived two separately gauge-invariant response tensors for these disordered superconductors in the presence of a supercurrent.

Im[σ] in the limit of extreme disorder. The imaginary part of the conductivity contains important information about the superfluid density. This is plotted in Fig. 3 along with the real counterpart for a more highly disordered system. With increasing disorder we have seen that the Higgs contribution becomes more dominant. There is also a sharpening of the

Higgs features in this dirty limit, as impurity effects tend to wash out the anisotropy in \mathbf{Q} , which is responsible for damping and pairbreaking, there by leading to a restoration of Anderson's theorem³⁴.

Particularly interesting is a downturn with decreasing ω in the imaginary part of the anisotropic conductivity. This directly reflects a depression in the superfluid density contribution which necessarily varies as $-1/\omega$ and appeared earlier in Eqs. 13 and 15. Although it was not discussed in any detail, experimental evidence for this downturn can be found in Ref. 11 in their Methods section.

Conclusions. An important contribution of this paper is to show how to separate the Higgs mode from the quasi-particle contributions to the conductivity, which have a similar frequency structure. We have shown that this similarity derives in part from the fact that there is an extra boost to the charge or quasi-particle conductivity arising from the amplitude of the order parameter. This, in turn, derives from pairbreaking effects made possible by the supercurrent in the presence of non-magnetic impurities. We have emphasized in this pa-

per that only in the limit of extreme disorder does this Higgs contribution dominate the conductivity, and this dominance pertains primarily to the real part of the conductivity.

By addressing a more extensive range of low frequencies, we are able to see new features in particular reflecting the supercurrent-derived reduction in the superfluid density which necessarily is present as a $1/\omega$ tail in the imaginary contribution. This tail arises from contributions from both the quasi-particle and Higgs modes. Interestingly, some indications of this effect seem to be present in experiments³⁵. We end by emphasizing that it will be of considerable interest to experimentally study cleaner films in future to arrive at a more systematic understanding of the very rich electrodynamic of the Higgs amplitude mode presented here.

Acknowledgment. We thank Andrew Higginbotham for very helpful discussions and Ryo Shimano for his communications. We also acknowledge the University of Chicago's Research Computing Center for their support of this work. R. B. was supported by the Department of Physics and Astronomy, Dartmouth College.

-
- ¹ Y. Nambu, *Physical Review* **117**, 648 (1960).
² J. Goldstone, *Il Nuovo Cimento (1955-1965)* **19**, 154 (1961).
³ G. Rickayzen, *Phys. Rev.* **115**, 795 (1959).
⁴ R. Parks and P. Martin, *Superconductivity Vols. 1, 2* (American Institute of Physics, 1970).
⁵ P. W. Anderson, *Physical Review* **130**, 439 (1963).
⁶ P. W. Higgs, *Physical review letters* **13**, 508 (1964).
⁷ G. S. Guralnik, C. R. Hagen, and T. W. Kibble, *Physical Review Letters* **13**, 585 (1964).
⁸ F. Englert and R. Brout, *Physical review letters* **13**, 321 (1964).
⁹ The Higgs mode and the amplitude mode are identical only in a charged theory.
¹⁰ D. Pekker and C. Varma, *Annu. Rev. Condens. Matter Phys.* **6**, 269 (2015).
¹¹ S. Nakamura, Y. Iida, Y. Murotani, R. Matsunaga, H. Terai, and R. Shimano, *Phys. Rev. Lett.* **122**, 257001 (2019).
¹² P. Littlewood and C. Varma, *Physical Review B* **26**, 4883 (1982).
¹³ D. Browne and K. Levin, *Physical Review B* **28**, 4029 (1983).
¹⁴ M. Papaj and J. E. Moore, *Phys. Rev. B* **106**, L220504 (2022).
¹⁵ P. J. D. Crowley and L. Fu, *Phys. Rev. B* **106**, 214526 (2022).
¹⁶ Z. Dai and P. A. Lee, *Physical Review B* **95**, 014506 (2017).
¹⁷ A. A. Abrikosov, I. Dzyaloshinskii, L. P. Gorkov, and R. A. Silverman, *Methods of quantum field theory in statistical physics* (Dover, New York, NY, 1975).
¹⁸ A. Moor, A. F. Volkov, and K. B. Efetov, *Phys. Rev. Lett.* **118**, 047001 (2017).
¹⁹ T. Kubo, *Physical Review Applied* **22**, 044042 (2024).
²⁰ T. Kita, *Physical Review B* **64**, 054503 (2001).
²¹ C. Gorini, P. Schwab, R. Raimondi, and A. L. Shelankov, *Physical Review B Condensed Matter and Materials Physics* **82**, 195316 (2010).
²² F. Yang and M. Wu, *Physical Review B* **106**, 144509 (2022).
²³ I. O. Kulik, O. Entin-Wohlman, and R. Orbach, *Journal of Low Temperature Physics* **43**, 591 (1981).
²⁴ K. Maki, *Progress of Theoretical Physics* **29**, 10 (1963).
²⁵ K. Maki, *Progress of Theoretical Physics* **29**, 333 (1963).
²⁶ Y. Zha, K. Levin, and D. Z. Liu, *Phys. Rev. B* **51**, 6602 (1995).
²⁷ R. Boyack and P. L. e. S. Lopes, *Phys. Rev. B* **101**, 094509 (2020).
²⁸ The formalism can be easily generalized to include Coulomb fluctuations. Since we are mainly concerned with frequency comparable to Δ , we focus on order-parameter fluctuations.
²⁹ H. Guo, C.-C. Chien, and Y. He, *Journal of Low Temperature Physics* **172**, 5 (2013).
³⁰ R. Boyack, B. M. Anderson, C.-T. Wu, and K. Levin, *Phys. Rev. B* **94**, 094508 (2016).
³¹ D. C. Mattis and J. Bardeen, *Physical Review* **111**, 412 (1958).
³² See supplementary materials.
³³ R. Boyack, C.-T. Wu, B. M. Anderson, and K. Levin, *Phys. Rev. B* **95**, 214501 (2017).
³⁴ P. W. Anderson, *Journal of Physics and Chemistry of Solids* **11**, 26 (1959).
³⁵ Private Communication with Ryo Shimano.

Supplemental Material for The Higgs- Amplitude mode in the optical conductivity in the presence of a supercurrent: Gauge invariant formulation

Ke Wang,^{1,2} Rufus Boyack,³ and K. Levin¹

¹*Department of Physics and James Franck Institute, University of Chicago, Chicago, Illinois 60637, USA*

²*Kadanoff Center for Theoretical Physics, University of Chicago, Chicago, Illinois 60637, USA*

³*Department of Physics and Astronomy, Dartmouth College, Hanover, New Hampshire 03755, USA*

S1. CHARACTERIZING THE HIGGS

Fig. S1 plots the isolated Higgs contribution. One can see that this is consistent with the f-sum rule, and that it has a negative weight contribution to the conductivity. There is, as well a negative delta function component representing the depression in the superfluid density associated with the Higgs.

Fig. S2 plots the imaginary part of the conductivity for moderate disorder which has an interesting feature directly reflecting the negative superfluid density contributions discussed in maintext. For $\omega > \Delta$ (experimentally accessible regime), the theoretical results align well with the measurements, although this system is noticeably less disordered than in experiment. Around $\omega \sim 2\Delta$, σ_{charge} exhibits greater asymmetry than σ_{Higgs} . This reflects the fact that the overall asymmetry of σ is due to σ_{charge} rather than the Higgs contribution. At lower frequencies $\omega < \Delta$, we observe that the curve begins to reflect the negative superfluid contribution $\propto -1/\omega$.

Disorder plays an important role in the Higgs contributions. The Higgs propagator is defined as $G_H(k) = (S_{11}(k) + 2/g)^{-1}$. We now examine its fundamental properties. In the clean limit, it can be shown that $G_H(\omega, \mathbf{k} = 0) \propto 1/\sqrt{4\Delta^2 - \omega^2}$, which exhibits a branch-cut singularity, indicating that the Higgs mode is undamped. When a disorder potential is introduced, damping effects arise, and this can be parameterized using a phenomenological form:

$$G_H^{-1}(\omega) = \sqrt{4\Delta^2 - (\omega + i\lambda)^2}. \quad (\text{S1})$$

Here, λ denotes the damping rate of the Higgs mode which we will address more microscopically. In the two asymptotic limits ($\tau\Delta \ll 1$ and $\tau\Delta \gg 1$), we confirm the form of Eq. S1 and identify the scaling properties: $G_H^{-1}(2\Delta) \propto \sqrt{Q^2}/\tau$ for $\tau\Delta \gg 1$ and $G_H^{-1}(2\Delta) \propto \sqrt{k_F^2 \Delta Q^2 \tau}$ for $\tau\Delta \ll 1$. Here the coefficients of proportionality are complex. Below we will use these properties to address interesting properties of the calculated conductivity. Both the charge and Higgs components of the conductivity contain anisotropic (\mathbf{Q} -dependent) tensor contributions. These components contribute distinctly, and the value of τ significantly affects the relative strength of their contributions.

These disorder dependent phenomena depicted in Fig. 2 of the maintext can be explained as follows. $\text{Re}\sigma_{\text{charge}}$ captures the excitations of fermionic pairs. In the presence of disorder, the fermion lifetime scales as $\sim \tau$, and the two-particle propagator behaves as $G^{(2)}(2\Delta) \sim \tau$. By contrast, the Higgs mode exhibits different behavior: in cleaner samples, $G_H(2\Delta) \sim \sqrt{\tau}$. Consequently, when $\tau\Delta \gg 1$, the resonant peak from the two-particle contribution naturally dominates over the Higgs peak. However, in the dirty limit, the peak of $G^{(2)}(2\Delta) \sim \tau$ becomes significantly weaker, while $G_H(2\Delta) \sim 1/\sqrt{\tau}$ forms a sharp

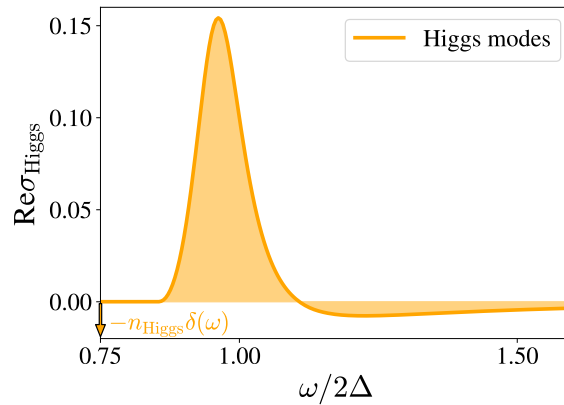


FIG. S1. (Color online). Plot of $\text{Re}\sigma_{\text{Higgs}}(\omega)$ in units of $\sigma_0 = e^2 m k_F / (2\pi^2 \hbar)$. What is plotted here is the projection of the conductivity tensor along the \hat{Q} -direction. We take as typical parameters $\Delta\tau = 0.2$ and $\Delta/E_F = 0.2$. The Higgs component of the conductivity is characterized by two key features: a positive peak around 2Δ and a negative superfluid weight at $\omega = 0$.

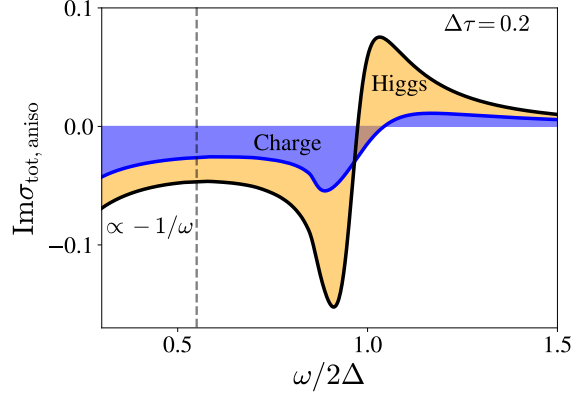


FIG. S2. (Color online). Plot of the imaginary part of $\sigma_{\text{tot, aniso}}$ in units of σ_0 . An asymmetric feature appears around $\omega = 2\Delta$, with the charge component being more asymmetric than the Higgs component. For $\omega < \Delta$, a negative asymptote proportional to $-1/\omega$ emerges, indicating a negative superfluid weight in this anisotropic component.

peak. Thus, when $\tau\Delta \ll 1$, the Higgs mode contribution to the peak becomes dominant over the charge component. It is important to note, though, that the tail of σ is primarily due to σ_{charge} , as small τ causes σ_{charge} to be more evenly distributed across all frequencies.

S2. DAMPING OF THE HIGGS MODE IN THE DIRTY LIMIT

The evaluation of the damping rate of the Higgs mode reduces to computing $G_H^{-1} = S_{11} + 2/g$. We begin with S_{ij} with Matsubara frequency and zero momentum:

$$S(i\omega_0) = 2\pi T \sum_{ik_0} \left(1 - \frac{1}{2\pi\tau} M(i\omega_0, i\omega_0 - ik_0) E^{33} \right)^{-1} M(i\omega_0, i\omega_0 - ik_0). \quad (\text{S2})$$

The matrix M is given by $M_u = \pi(f_1\tau_3 + if_2\tau_1 + f_3)$, where f_σ is defined by

$$f_1 = \left\langle \frac{1}{\tilde{r} + \tilde{r}'} \right\rangle_x, \quad f_2 = - \left\langle \frac{\tilde{\Delta}'\tilde{z} + \tilde{\Delta}\tilde{z}'}{(\tilde{r} + \tilde{r}')\tilde{r}\tilde{r}'} \right\rangle_x, \quad f_3 = \left\langle \frac{\tilde{\Delta}\tilde{\Delta}' \mp \tilde{z}\tilde{z}'}{(\tilde{r} + \tilde{r}')r'} \right\rangle_x. \quad (\text{S3})$$

Here, $\tilde{z} = \tilde{\omega}_0 + isx$, and $\langle \dots \rangle_x$ denotes $\int_{-1}^{+1} \dots dx/2$, with $s = v_F Q$ and $\tilde{r} = \sqrt{\tilde{z}^2 + \tilde{\Delta}^2}$. Note that $\tilde{\omega}_0$ and $\tilde{\Delta}$ need to be determined self-consistently from

$$\tilde{\omega}_0 - \omega_0 = \frac{t_+ - t_-}{d}, \quad \tilde{\Delta} - \Delta = \frac{\Delta}{d} \log \left(\frac{t_+ + \tilde{\omega}_+}{t_- + \tilde{\omega}_-} \right). \quad (\text{S4})$$

Here $\tilde{\omega}_\pm = \tilde{\omega}_0 \pm ik_F Q$, $t_\pm = \sqrt{\tilde{\omega}_\pm^2 + \tilde{\Delta}^2}$, and $d = 4ik_F Q\tau$, where τ is the impurity scattering time. Similarly, $\tilde{\omega}'$ and $\tilde{\Delta}'$ are derived from $\omega_0 - k_0$. Consequently, the expression for S_{11} simplifies to

$$S_{11} = 2\pi T \sum_{p_0} \frac{f_3 - [f_1 + D/2\tau]}{1 - f_1/\tau - D/4\tau^2}, \quad D = f_2^2 + f_3^2 - f_1^2. \quad (\text{S5})$$

Here, $D = 0$ if $Q = 0$. The evaluation of f_σ involves an angular average over x . In the $\tau\Delta < 1$ limit, f_σ is of the order τ , allowing the use of the integrand function at $x = 0$ as an approximation for f_σ . The deviation from the $x = 0$ value is minor, on the order of $O(v_F^2 Q^2 \tau^3)$. Thus, in the dirty limit, we approximate

$$G_H^{-1} = \int_C \frac{d\omega_0}{e^{i\beta\omega_0} + 1} \left[\frac{(\tilde{\Delta}\tilde{\Delta}' - \tilde{\omega}_0\tilde{\omega}_0')/\tilde{r}\tilde{r}' - 1}{\tilde{r} + \tilde{r}' - 1/\tau} + \frac{1}{r} \right]. \quad (\text{S6})$$

Here, C represents a contour encircling the real axis, $r = \sqrt{\omega_0^2 + \Delta^2}$, and \tilde{r} is evaluated at $x = 0$ in this integral, namely $\sqrt{\tilde{\omega}_0^2 + \tilde{\Delta}}$. In the dirty limit, we find:

$$\sqrt{\tilde{\omega}_0^2 + \tilde{\Delta}} \simeq \sqrt{\omega_0^2 + \Delta^2} + \frac{1}{2\tau} + \frac{k_F^2 Q^2 \tau \Delta^2}{3(\Delta^2 + \omega_0^2)}. \quad (\text{S7})$$

Note that $\sqrt{\tilde{\omega}_0^2 + \tilde{\Delta}} \rightarrow \sqrt{\omega_0^2 + \Delta^2} \eta$ as $\tau \rightarrow 0$, with $\eta = 1 + 1/2\tau\sqrt{\omega_0^2 + \Delta^2}$, typically observed in dirty BCS systems. Using Eq. S7, we solve

$$\tilde{\omega}_0 = \omega_0 \eta + \frac{1}{3} \frac{\omega_0 \Delta^2}{(\Delta^2 + \omega_0^2)^2} k_F^2 Q^2 + O(\tau), \quad \tilde{\Delta} = \Delta \eta - \frac{1}{3} \frac{\omega_0^2 \Delta}{(\Delta^2 + \omega_0^2)^2} k_F^2 Q^2 + O(\tau). \quad (\text{S8})$$

Interestingly, z deviates from the dirty BCS value by a constant term proportional to Q^2 even as $\tau \rightarrow 0$.

At zero temperature, we replace the contour integral with a real-axis integral and expand based on Eqs. S7 and S8:

$$\tilde{r} + \tilde{r}' - 1/\tau = r + r' + \frac{k_F^2 Q^2 \tau \Delta^2}{3} \left(\frac{1}{r^2} + \frac{1}{r'^2} \right), \quad (\text{S9})$$

$$\frac{\tilde{\Delta} \tilde{\Delta}' - \tilde{\omega}_0 \tilde{\omega}_0'}{\tilde{r} \tilde{r}'} \simeq \frac{\Delta \Delta - \omega_0 \omega_0'}{r r'} + 2\tau k_F^2 Q^2 \frac{(\Delta_0^2 + \omega_0 \omega_0')}{3r r'} \left(\frac{\Delta \omega_0}{r^3} + \frac{\Delta \omega_0'}{r'^3} \right). \quad (\text{S10})$$

Consequently, performing the integral in Eq. S6 yields:

$$G_B^{-1}(i\omega_0) \simeq \sqrt{\omega_0^2 + 4\Delta^2} + 2 \frac{k_F^2 q^2 \tau \Delta_0^2}{\sqrt{4\Delta_0^2 + k_0^2}} b(\omega_0). \quad (\text{S11})$$

Here, $b(\omega_0)$ represents a complex function obtained from the integral. The function $b(\omega_0)$ is analytic in the complex plane, except for branch cuts along the imaginary axis, where its values are bounded by $|\omega_0|$. One can rewrite Eq. S11 in a "non-perturbative" form:

$$G_B^{-1}(i\omega_0) \simeq \sqrt{k_0^2 + 4\Delta^2 + k_F^2 q^2 \tau \Delta_0^2 b(\omega_0)}. \quad (\text{S12})$$

Finally, we perform the analytical continuation $i\omega_0 \rightarrow \Omega + i\delta$ with $\delta > 0$:

$$G_B^{-1}(\Omega + i\delta, 0) \simeq \sqrt{4\Delta^2 - \Omega^2 + k_F^2 Q^2 \tau b(-i\Omega + \delta)}. \quad (\text{S13})$$

Thus, we confirm the form of Eq. S1 within the dirty limit, indicating that the asymptotic scaling of the damping rate λ at $\Omega = 2\Delta$ is proportional to $k_F^2 Q^2 \tau$.

S3. IMPURITY EFFECTS ON THE CURRENT OPERATOR

The bare current operator for a superconductor carrying a uniform supercurrent is given by

$$j(\mathbf{p}) = \frac{\mathbf{p}\tau_0 + \mathbf{Q}\tau_z}{m}, \quad \hat{j}(\mathbf{k}) = \sum_{\mathbf{p}} \Psi^\dagger(\mathbf{p} - \mathbf{k}/2) j(\mathbf{p}) \Psi(\mathbf{p} + \mathbf{k}/2). \quad (\text{S14})$$

The effects of disorder renormalize the current operator as follows:

$$\Gamma_J(\mathbf{p}) = j(\mathbf{p}) + n_i \sum_{\mathbf{p}'} |V_n(\mathbf{p} - \mathbf{p}')|^2 \tau_3 G_{\mathbf{p}'}(\omega) \Gamma_J(\mathbf{p}') G_{\mathbf{p}'}(\omega - \Omega) \tau_3. \quad (\text{S15})$$

Here, V represents the impurity potential. We consider non-magnetic impurities as $V(\mathbf{r})\tau_z$ and assume a contact interaction for this disorder. An important observation is that the vertex can always be split into two parts:

$$\Gamma_J(\mathbf{p}) = \frac{\mathbf{p}\Lambda_0 + \mathbf{Q}\Lambda_1}{m}. \quad (\text{S16})$$

Here, Λ_0 and Λ_1 are two 2×2 matrices. For a contact potential, one can prove $\Lambda_0 = \tau_0$. This follows because the integration over $G\Gamma_j G$ in p' only provides corrections along the \mathbf{Q} -direction. Thus, we have $\Lambda_0 = \tau_0$. The matrix Λ_1 , associated with \mathbf{Q} , satisfies the equation:

$$\mathbf{Q}\Lambda_1 = \mathbf{Q}\tau_z + \frac{1}{2\pi\tau} \int \frac{dx}{2} \int d\xi_{p'} \tau_3 G_{\mathbf{p}'}(\omega) (\mathbf{p}'\tau_0 + \mathbf{Q}\Lambda_1) G_{\mathbf{p}'}(\omega - \Omega) \tau_3. \quad (\text{S17})$$

Projecting Eq. S17 along \mathbf{Q} it follows that

$$\Lambda_1 = \tau_z + \frac{1}{2\pi\tau} \frac{p_F}{Q} \int d\xi_p \frac{dx}{2} \tau_3 G_{\mathbf{p}'}(\omega) x \tau_0 G_{\mathbf{p}'}(\omega - \Omega) \tau_3 + \frac{1}{2\pi\tau} \int d\xi_p \frac{dx}{2} \tau_3 G_{\mathbf{p}'}(\omega) \Lambda_1 G_{\mathbf{p}'}(\omega - \Omega) \tau_3. \quad (\text{S18})$$

Note that the second term does not include Λ_1 . We define c_0, c_1 , and Π_l as follows:

$$c_0 + c_1 \tau_1 \equiv \frac{1}{2\pi\tau} \frac{p_F}{Q} \int_{-1}^1 \frac{dx}{2} x \tau_3 \Pi_0 \tau_3, \quad \text{and} \quad \Pi_l \equiv \int d\xi_p G_{\mathbf{p}'}(\omega) \tau_l G_{\mathbf{p}'}(\omega - \Omega). \quad (\text{S19})$$

Thus, Eq. S18 can be rewritten as

$$\Lambda_1 = c_0 + c_1 \tau_x + \tau_z + \frac{1}{2\pi\tau} \int d\xi_p \frac{dx}{2} \tau_3 G_{\mathbf{p}'}(\omega) \Lambda_1 G_{\mathbf{p}'}(\omega - \Omega) \tau_3. \quad (\text{S20})$$

Expanding Λ_1 in Pauli matrices, it follows that $\Lambda_1 = \sum_i B_i \tau_i$, and we find $\mathbf{B} = \mathbf{c} \left(1 - \frac{1}{2\pi\tau} M E^{33}\right)^{-1}$. Here we define vectors $\mathbf{B} = (B_0, B_1, B_2, B_3)$, $\mathbf{c} = (c_0, c_1, 0, 1)$ while M and E^{33} are specified in Eq. 21 of the main text. Finally, the renormalized current vertex within the supercurrent framework is

$$\Gamma_j(\mathbf{p}; \omega, \omega') = \frac{\mathbf{p}\tau_0}{m} + \frac{\mathbf{Q}\tau_i}{m} \left[\mathbf{c} \left(1 - \frac{1}{2\pi\tau} \langle M \rangle E^{33}\right)^{-1} \right]_i. \quad (\text{S21})$$